

COMPARISON OF PROPERTIES OF CELLULOSE NANOMATERIALS OBTAINED FROM SUNFLOWER STALKS

EKREM DURMAZ and SAIM ATEŞ

*Kastamonu University, Faculty of Forestry, Department of Forest Industrial Engineering,
37150, Kastamonu, Turkey*

✉ *Corresponding author: E. Durmaz, edurmaz@kastamonu.edu.tr*

Received March 23, 2021

This study aimed to investigate the usability of sunflower stalks, which is one of the most significant agricultural residues in Turkey, in the production of cellulose nanomaterials (CNMs). Cellulose nanofibrils (CNFs) and cellulose nanocrystals (CNCs) were produced by using a grinding method and acid hydrolysis, respectively. The average width and length of CNCs were found as 13.91 ± 3.09 nm and 60.44 ± 21.06 nm, respectively. Besides, the average width of CNFs was determined as 15.03 ± 3.68 nm. The crystallinity index of CNFs and CNCs was determined as 82.64% and 83.09%, respectively. Although the main thermal degradation stage of CNCs started at higher temperature than that of CNFs, the latter were more stable than CNCs at high temperatures. Furthermore, the chemical bonds in the raw material, bleached fiber, CNCs and CNFs were investigated with FTIR analysis. Consequently, it was seen that sunflower stalks can be a suitable raw material for the production of CNMs.

Keywords: sunflower stalks, agricultural residues, cellulose nanofibrils, cellulose nanocrystals

INTRODUCTION

Cellulose is one of the essential constituents of the cell wall of lignocellulosic biomass and it has been used in industries such as paper and packaging,¹ textiles and foods,² pharmaceuticals and cosmetics,³ as well as adhesive industries⁴, for many years. Nevertheless, research efforts have been made to adapt cellulose to nanotech applications in the last decades.⁵ Due to their adjustable nature, cellulose nanomaterials (CNMs), alone or in combination with other polymers in the production of composites, have been extensively used in different areas, including composite films, packaging, paper, tissue engineering, bioprinting, textiles, regenerative medicine, optoelectronics, energy, environmental remediation, cosmetics, foods *etc.*,⁶⁻¹¹ owing to their outstanding properties, such as three-dimensional nano-structure, advanced mechanical strength, high crystallinity, high surface area, advanced hydrophilicity, biodegradability, biocompatibility and optical transparency.¹²⁻¹⁴

Cellulose nanomaterials are generally categorized into two basic groups related to their production process, *i.e.*, cellulose nanocrystals (CNCs) and cellulose nanofibrils (CNFs). According to ISO/TS 20477,¹⁵ cellulose nanocrystals are also called nanocrystalline cellulose (NCC) or cellulose nanowhiskers (CNWs), while cellulose nanofibrils are also referred to as nanofibrillated cellulose (NFC), nanofibrillar cellulose (NFC) or cellulose nanofibre (CNF), different terminology being used in the literature.

CNFs are manufactured by a high-shear mechanical treatment of purified and bleached biomass pulp using a microfluidizer, high-pressure homogenizer or grinder. In addition, some mechanical, chemical or enzymatic pretreatments are applied to ease the defibrillation in the production of CNFs. Contrary to CNFs, CNCs are usually achieved by strong acid hydrolysis of purified and bleached biomass pulp. As a result of these various processes, CNCs exhibit rice-like shape, with only crystalline zones, whereas CNFs have spaghetti-like structure, with both crystalline and amorphous zones.^{1,16} The width and length of CNFs are 3-100 nm and 100 μ m, respectively, while their aspect ratio is usually greater than 10. Likewise, the width and length of CNCs are 3-50 nm and from 100 nm to several μ m, with an aspect ratio of 5-50.¹⁵

Different types of wood pulp, such as bleached kraft pulp,^{17,18} wood flour,¹⁹ sulphite pulp²⁰ and bleached sulphite pulp,²¹ have been used for production of CNMs. Also, some annual plants and agricultural wastes, such as bamboo, cotton, sisal, jute, hemp, wheat straw, rice straw, kenaf, sugar beet pulp, bagasse, banana rachis, swede root, coconut husk and pea hull, as well as tunicate and some

bacteria, such as *Acetobacter*, *Agrobacterium*, *Alcaligenes*, *Escherichia*, *Pseudomonas*, *Azotobacter*, *Rhizobium* or *Sarcina* etc., have been used as raw materials in production of CNCs and CNFs.²²⁻²⁴

Sunflower is one of the most commonly grown agricultural plants in the world due to its oil and seed. The global production of sunflower reached 56 million tons, while in Turkey, it amounted to 2.1 million tons in 2019. Demirel²⁵ investigated 20 different sunflower varieties and found their mean harvesting index as 0.39. It means that, in Turkey alone, about 3.28 million tons of potential waste sunflower biomass, made up of stalks, heads and leaves, is available, while at present, this residue remains in the fields after harvesting or is used as combustible material and animal feed. As one of the most cultivated agricultural crops in Turkey, the cultivation area of sunflower increased by 8.3%, compared to the previous season, and reached about 780 thousand hectares. Moreover, the 3-7 tons of dry matter/ha of sunflower biomass are produced annually,²⁶ which makes these lignocellulosic residues a major low-cost source of value-added products, such as different kind of board, paper and nanomaterials.

In the present study, the possibility of producing CNMs from sunflower stalks, an agricultural residue, which is currently underused, is investigated. Some properties of CNFs and CNCs are evaluated and compared with each other. Thus, the optimum process and the most usable form of cellulose nanomaterials produced from sunflower wastes are determined.

EXPERIMENTAL

Materials

In this study, sunflower stalk wastes were collected from Samsun province of Turkey. The sunflower leaves and heads were removed and the remaining stalks were chopped by a knife to 2-3 cm length and 1-2 cm width.

All the chemicals used for the experiments and the trials: ethanol (96%), NaClO₂ (80% pure), glacial acetic acid (99%), hydrochloric acid (37%), NaOH, sulphuric acid (97%), nitric acid (70%) and chloroform, were supplied by Sigma Aldrich, USA. NanoVan for preparing the samples for TEM analysis was purchased from Nanoprobes Company, USA.

Methods

Determination of chemical composition of sunflower stalk wastes

Sunflower stalk wastes were cut to small sizes to grind in a Willey-type mill. The obtained sunflower stalk flour was sifted in 40 and 60 mesh sieves. The powders obtained from the 60 mesh sieve were used as experimental samples in the tests according to TAPPI T257.²⁷ All of the experiments were conducted according to TAPPI standards. Extractives, holocellulose, α -cellulose, lignin and ash contents, hot and cold water as well as 1% NaOH solubilities were determined according to TAPPI T204,²⁸ Wise Chlorite Method,²⁹ TAPPI T203,³⁰ TAPPI T222,³¹ TAPPI T211,³² TAPPI T207³³ and TAPPI T212,³⁴ respectively.

The chemical composition of the sunflower stalk wastes was determined, and the maceration and bleaching processes in the production of CNFs and CNCs were conducted at Kastamonu University, Faculty of Forestry, Department of Forest Industrial Engineering Laboratories, while the production of CNFs and CNCs was performed in the labs of the Department of Forest Biomaterials, College of Natural Resources, North Carolina State University.

Production of cellulose nanofibrils (CNFs) and cellulose nanocrystals (CNCs) from sunflower stalk wastes

Preparation of sunflower stalks

The sunflower stalks were subjected to maceration and bleaching processes before the production of CNFs and CNCs. Sized samples were macerated according to the method of Mahesh *et al.*³⁵ Fibrillated samples were bleached according to the Wise Chlorite Method,²⁹ similarly to the method used for determining the holocellulose content. The delignification process was conducted by the Wise Chlorite Method and the lignin from the raw material was removed. Thereby, sunflower stalk wastes were made ready for production of CNFs and CNCs. Besides, the moisture content of the fiber samples was determined as 14.4%.

Production of cellulose nanofibrils (CNFs)

CNFs were produced from the bleached sunflower stalk fibers according to the modified method described by Gu *et al.*³⁶ In brief, firstly the fibers were separated with 3 replicates at 15000 rpm in a lab-style pulp disintegrator. Then, the pulp was beaten with a PFI mill at 20000 rpm during 20 min according to TAPPI T248.³⁷ Canadian standard freeness (CSF) of the beaten pulp and bleached fibers was determined according to TAPPI T227.³⁸ These values were found as 34 CSF for beaten pulp and 820 CSF for bleached fibers. After that, the pulp suspension was homogenized with a lab-style mechanical stirrer during 30 min. CNFs were produced by using 5

times grinding processes in a Supermasscolloider grinder (MKCA6-5J, Masuko Sangyo, Japan). The solid content of the produced CNFs was 2%. The parameters used in the production of CNFs are shown in Table 1.

The produced CNFs were gel-like and were stored in plastic containers at 4 °C. A few drops of chloroform were added to the CNFs samples to prevent any bacterial or fungal growth.

Table 1
Parameters used in the production of CNFs

Number of grinding repetitions	No-load operating power (kW)	Grinding operating power (kW)	Speed (rpm)	Distance between discs (μm)	Treatment time
1	0.2	0.27	750	-50	10 min 56 s
2	0.2	0.28	750	-100	14 min 10 s
3	0.2	0.28	750	-100	16 min 17 s
4	0.2	0.30	750	-200	47 min 30 s
5	0.2	0.32	750	-200	1 h 35 min 33 s

Production of cellulose nanocrystals (CNCs)

CNCs were obtained from the bleached sunflower stalk fibers according to the modified method by Korolovych *et al.*³⁹ In this method, sulfuric acid in 64% concentration (H₂SO₄) was used and the sample/acid ratio was determined as 10 g/100 mL. In short, acid hydrolysis was performed with a 2-L 3-necked glass flask under a fume hood at 45-50 °C during 1 hour. A Teflon propeller mixer, a thermometer and a cooler system were attached to this flask. The system was placed in a silicone oil bath and on the heater. The acid hydrolysis reaction was stopped by adding the 5 fold amount of distilled water of the sample/acid volume in the system to the glass flask. The solution in the flask was transferred to centrifuge tubes. Centrifugation was conducted at 4400 rpm during 10 minutes and this process was repeated 5 times for each sample. After each repetition, the supernatants in the tubes were replaced with fresh distilled water. After centrifugation, the supernatant and the precipitate in the tubes were homogenized by mixing with Ultra Turrax at 10000 rpm for 2-3 min. A dialysis process was applied to homogenized CNCs solutions. The dialysis process reduces the acid content of CNCs by means of osmotic pressure. The CNCs placed in dialysis tubes, with molecular weights of 12000-14000 Daltons, were immersed in distilled water and kept there until their pH reached 7 (approximately a week). The used distilled water was reloaded every day. After the pH level of CNCs reached almost 7, the second centrifugation was performed, with two repetitions with the same parameters, to remove residual acid in the solutions. Then, mixing with an Ultra Turrax and ultrasonication with a Branson Sonicator were done to separate the aggregated CNCs in the solutions. The ultrasonication process was conducted at 60 kHz for 1 min. The processes conducted in the production of CNMs are summarized in Figure 1.

Characterization of cellulose nanofibrils (CNFs) and cellulose nanocrystals (CNCs)

In the characterization of sunflower stalk CNFs and CNCs, an optical microscope (OM), a scanning electron microscope (SEM) and a scanning transmission electron microscope (S/TEM) were used for observing morphological properties. X-ray diffraction (XRD) was performed for assessing crystallinity, Fourier transform infrared spectroscopy (FTIR) – for evaluating chemical bonds, thermogravimetric analysis (TGA) and differential scanning calorimetry (DSC) – for determining thermal properties, as well as turbidity and zeta potential. OM, SEM, S/TEM, turbidity and zeta potential analyses were conducted on CNCs and CNFs in solution form. On the one hand, freeze-dry CNC and CNF samples were used for XRD, FTIR, TGA and DSC analyses. In the freeze-drying process, CNF and CNC solutions in centrifuge tubes were submerged into a liquid nitrogen container for 15 min. Then, these samples were put in freeze-drying equipment (Labconco, FreeZone 2.5 Liter Benchtop Freeze Dryer, USA). The samples were treated at -55 °C and the pressure of 0.015-0.025 mBar during 4 days.

Determination of turbidity and zeta potential of CNFs/CNCs and energy consumption in the production of CNFs

The turbidity of CNFs and CNCs was determined with a turbidity meter (LaMotte 2020wi Turbidity Meter, USA) and a zetasizer (Malvern Zetasizer, UK) was used for determining the zeta potential of CNFs and CNCs. The CNF and CNC solutions were diluted to 0.1% concentration before these experiments.

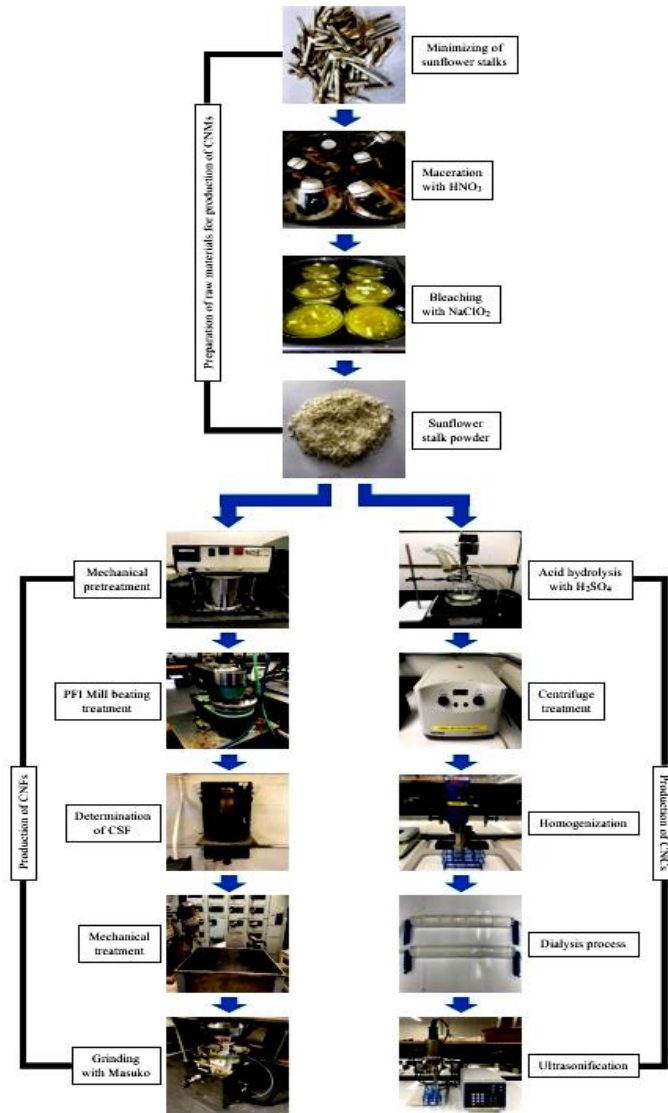


Figure 1: Processes conducted in the production of CNMs

Energy consumption in the production of CNFs was calculated with the following formula:⁴⁰

$$E_s[\text{kWhkg}^{-1}] = \frac{P_s[\text{kW}] \times t[\text{h}]}{w_{\text{CNF}}[\text{kg}]} \quad (1)$$

where E_s = specific energy consumption, P_s = operating power surplus, which was determined by subtracting the no-load operating power from the total operating power during grinding, t = sampling time, w_{CNF} = weight of dry CNFs processed for a certain time t .

Determination of sulfur content of CNCs

Conductometric titration of CNCs was carried out depending on the change in pH and the amount of NaOH. The slope, obtained from the titration values, was used to determine the sulfur content of CNCs. The procedure for determining the sulphur content was carried out according to Dong *et al.*,⁴¹ and the sulphur content was calculated with the following formula:

$$\%S = \frac{V_{\text{NaOH}} \times C_{\text{NaOH}} \times M_w(S)}{m_{\text{susp}} \times C_{\text{susp}}} \times 100\% \quad (2)$$

where $\%S$ = sulfur content, m_{susp} = mass of the cellulose nanocrystal suspension, C_{susp} = concentration (mass %) of the cellulose nanocrystal suspension, V_{NaOH} = volume of NaOH required for neutralization, C_{NaOH} = concentration of NaOH required for neutralization, M_w = atomic mass of sulphur.

Optical microscopy analysis

The morphological properties of CNCs and CNFs were investigated by an optical microscope firstly, before SEM and S/TEM analyses. The morphologies of the samples taken from each of the 5 repetitions of the grinding

process applied in the production of CNFs were observed and the fibrillation degrees at each stage of the grinding process were determined. Optical analyses were done by using an Olympus Optical Microscope at 1000x magnification, together with NIS-Elements Microscope Imaging Software.

Scanning electron microscopy (SEM) analysis

The raw material, bleached fiber and CNF samples were characterized using a scanning electron microscope (SEM) (Quanta FEG 250, USA) at Mehmet Hakan Akyıldız Central Research Laboratory, Kastamonu University, Turkey, and a variable-pressure scanning electron microscope (VPSEM) (Hitachi S3200N, Japan), with an energy dispersive X-ray spectrometer, using an acceleration voltage of 15 kV, at Analytical Instrumentation Facility (AIF), North Carolina State University, USA. Before imaging of CNFs, the sample solution was diluted with water to 0.01% concentration, and then dried with a vacuum dryer.

Scanning transmission electron microscopy (S/TEM) analysis

CNF and CNC samples were monitored using a scanning transmission electron microscope (S/TEM) (Talos F200X, ThermoFisher, USA) at 200 kV, equipped with a four segment SuperX energy-dispersive X-ray spectroscopy (EDX) system, at North Carolina State University, USA. Before the analysis, CNFs were diluted with water to 0.05% concentration, while CNCs were diluted to 0.005% concentration.

X-ray diffraction (XRD) analysis

The crystallinity index (CI) determines the orientation of cellulose crystals in a fiber related to the fiber axis. The CI was found by using the wide angle X-ray diffraction (WAXD) counts at 2θ angle close to 22° and 18° . The peak at 22° indicates the crystalline part, whereas the peak at 18° states the amorphous part in cellulose materials. From these readings, the crystallinity index (CI) was calculated by using Equation (3):⁴²

$$CI (\%) = \frac{I_{22} - I_{18}}{I_{22}} \times 100 \quad (3)$$

where I_{22} and I_{18} stand for the counter readings at 2θ close to 22° and 18° , respectively.

The crystalline structures of the raw material, bleached fiber, CNFs and CNCs were identified by X-ray diffraction, using a Rigaku SmartLab XRD (Akishimashi, Japan) at Analytical Instrumentation Facility (AIF), North Carolina State University, USA, and a Bruker D8 Advance XRD (Germany) at Mehmet Hakan Akyıldız Central Research Laboratory, Kastamonu University, Turkey. This analysis was operated by using a Cu target to generate X-rays using $K\alpha$ radiation (Cu $K\alpha$ radiation, $\lambda = 0.15418$ nm) in the range of 5 - 60° 2θ . The diffraction data were obtained using a step size and count time of 0.05° 2θ and 3 s/step, respectively.

Fourier transform infrared spectroscopy (FTIR) analysis

The chemical bond structures of all the samples were determined by using a FTIR spectrometer (Perkin Elmer Frontier, USA), with a Universal ATR sampling accessory, at the Chemical Analysis and Spectroscopy Laboratory, Department of Forest Biomaterials, North Carolina State University, USA. Each sample was scanned twice between 4000 - 650 cm^{-1} wavelengths, with a scanning resolution of 4 cm^{-1} .

Thermogravimetric analysis (TGA)

The thermal properties of the raw material, bleached fiber, freeze-dried CNF and freeze-dried CNC samples were investigated with TGA analysis (TGA Q500, TA Instruments, USA) at the Chemical Analysis and Spectroscopy Laboratory, Department of Forest Biomaterials, North Carolina State University, USA. TGA analysis was performed under air and nitrogen gas flow at a temperature of 30 - 600 $^\circ\text{C}$, using a temperature ramp of 10 $^\circ\text{C min}^{-1}$.

Differential scanning calorimetry (DSC) analysis

In addition to TGA analysis, DSC analysis (DSC2000, TA Instruments, USA) was also conducted to analyze the thermal properties all the samples, at the Chemical Analysis and Spectroscopy Laboratory, Department of Forest Biomaterials, North Carolina State University, USA. DSC analysis was conducted in nitrogen atmosphere between 30 - 400 $^\circ\text{C}$ using a temperature ramp of 10 $^\circ\text{C min}^{-1}$.

RESULTS AND DISCUSSION

Chemical composition of sunflower stalks

The chemical composition of the sunflower stalks used as raw material in this study was determined according to TAPPI standards and the results are shown in Table 2, in comparison with other previously reported findings. According to the data in Table 2, the contents of holocellulose and lignin, which are the basic components of a cellulosic material, were found as 64.14% and 16.07%,

respectively. The alpha-cellulose content, which is important in the production of CNMs, was found relatively high (49.57%).

Turbidity and zeta potential of CNFs/CNCs and energy consumption in the production of CNFs

The relation between turbidity, zeta potential and energy consumption with the number of grinding repetitions in the production of CNFs is shown in Figure 2. The turbidity of CNFs decreased when the number of grinding repetitions in the production of CNFs increased. The turbidity value, which was 38.373 FNU for the first grinding, reduced to 14.31 FNU, decreasing by 62.70% by the end of the fifth grinding, when CNFs were obtained. These results prove that, as the turbidity value of CNFs decreases, the dimensions of the fibers in the CNF solution get closer to the nanoscale dimensions.⁴⁵ Pacaphol *et al.*⁴⁶ produced CNFs using a microfluidizer and repeating this mechanical process for different times in their study. According to the obtained results, it was determined that the turbidity values diminished from 490 NTU to 173 NTU, due to the decrease in the dimensions of the produced CNFs, with the increase in the number of repetitions of the mechanical process. In contrast to turbidity, as the number of grinding repetitions in the production of CNFs increased, the zeta potential of CNFs also rose. The zeta potential value, which was determined as -35.611 mV in the first grinding increased by 7.21% in the fifth grinding, where the fibers were converted to CNFs, and reached -38.18 mV. The reason for this was that, as the fibers approached the nano-dimensions, their surface area increased.⁴⁷⁻⁴⁹ Oh *et al.*⁵⁰ found that the zeta potential of larger microfibers varied between -11.6 mV and -25 mV, while the zeta potential of nanofibers varied between -12.7 mV and -26.7 mV.

The results in Figure 2 reveal that there was a direct relationship between released energy consumption and the number of grinding repetitions in the production of CNFs. The amount of consumed energy, which was calculated as 0.16 kWhkg⁻¹ in the first stage of the grinding process, increased by 1400% in the fifth grinding stage, where CNFs were produced, and it reached 2.4 kWhkg⁻¹. The reason for this increase in energy consumption was that the dimensions of the fibers in the grinder reduced gradually during the grinding stages and approached the nano-scale. Thus, these fibers, which reached nano-dimensions, were processed in the grinder much more. Josset *et al.*⁵¹ investigated the relation between energy consumption and the number of grinding repetitions (2, 4, 6, 8 and 10) in the production of CNFs, obtained from bleached wood pulp, recycled newspapers and wheat straw. They determined that, as the number of grinding repetitions in the production of CNF samples increased, in other words, as the samples reached the nano-scale, the energy consumption increased from 1 kWhkg⁻¹ to $5-7$ kWhkg⁻¹. In another study, Kriechbaum *et al.*⁴⁰ found the energy consumption in the production of CNFs from kraft and sulphite pulps as 0.12 kWhkg⁻¹, 0.44 kWhkg⁻¹ and 0.92 kWhkg⁻¹ for kraft pulp, as 0.12 kWhkg⁻¹, 0.39 kWhkg⁻¹ and 0.85 kWhkg⁻¹ for sulphite pulps when the number of grinding repetitions in the production increased.

The turbidity of the CNCs was determined as 1.02 FNU, while their zeta potential was found as -39.06 mV. As seen from the results, although zeta potential values were higher, the turbidity of CNCs was lower than that of CNFs by about 92%. This should have been due to the fact that the dimensions of the CNCs were smaller than the dimensions of the CNFs. Similarly, Ilyas *et al.*⁵² found the zeta potential of sugar palm CNFs with 21.37 nm width as -39.5 mV, while Ribeiro *et al.*⁵³ found the zeta potential of eucalyptus CNCs with 8.9 nm width as -45.23 mV. In addition, the changes in the parameters (acid concentration, hydrolysis time *etc.*) applied in the production of CNCs also affect the zeta potential of these nanoparticles. For example, El Achaby *et al.*⁴⁷ obtained CNCs from red algae by acid hydrolysis lasting for 30, 40 and 80 min. The length and diameter of CNCs decreased with the increase in acid hydrolysis time, whereas the zeta potential values increased. These values were determined as -25.17 mV, -28.25 mV and -30.71 mV for CNC₃₀, CNC₄₀ and CNC₈₀, respectively.

Table 2
Chemical composition of sunflower stalks

Raw material	Chemical composition							Solubility			References	
	Holocellulose (%)	Cellulose (%)	α -cellulose (%)	Lignin (%)	Silica (%)	Ash (%)	Alcohol-benzene (%)	Acetone (%)	1% NaOH	Hot water (%)		Cold water (%)
Sunflower stalk	64.14	-	49.57	16.07	-	8.09	7.66	-	35.93	19.69	16.87	This study
Sunflower stalk	66.85	47.8	44.2	14.43	0.44	7.99	7.48	4.86	50.05	24.26	21.08	(43)
Sunflower stalk	74.9	47.6	37.5	18.2	-	8.2	7.0	-	29.8	16.5	-	(44)

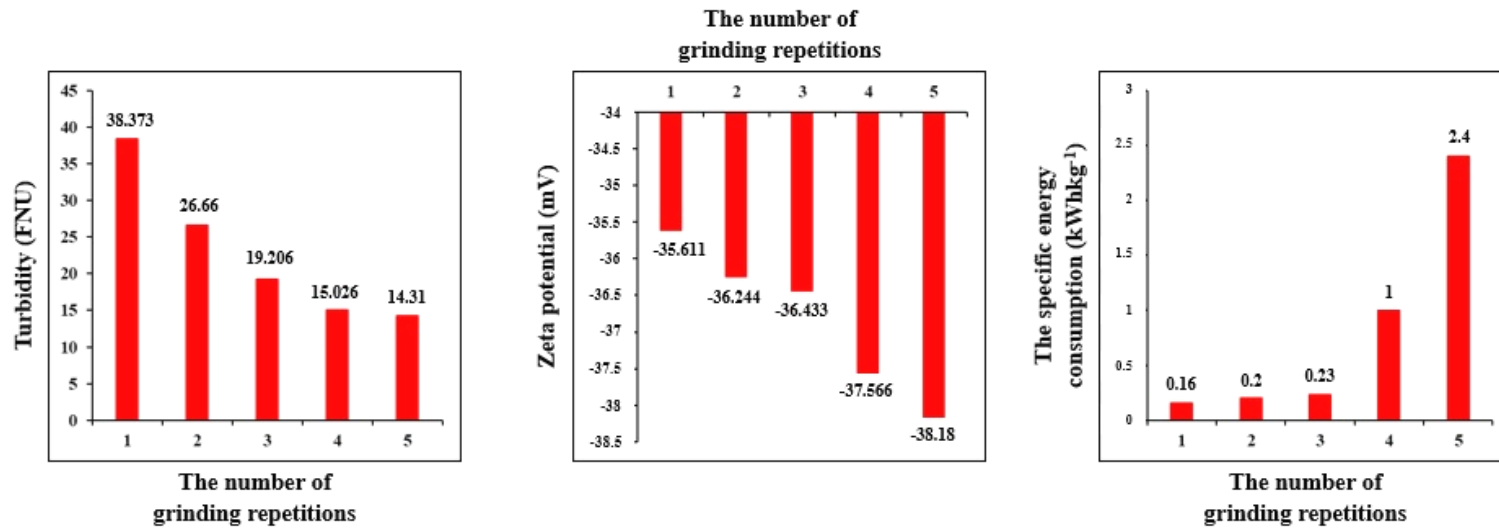


Figure 2: Relation between turbidity, zeta potential, energy consumption and the number of grinding repetitions in the production of CNFs (FNU: Formazin Nephelometric Unit)

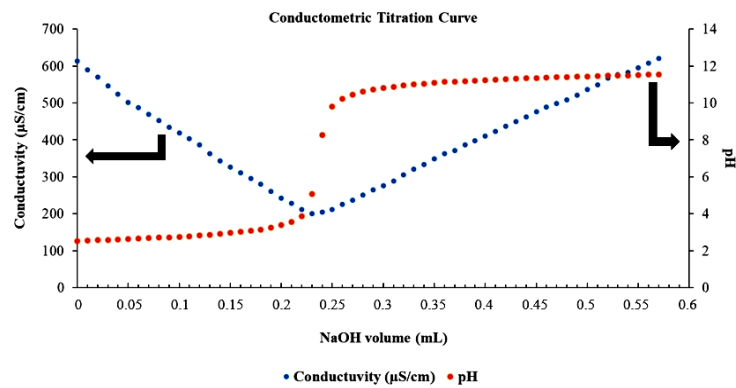


Figure 3: Conductometric titration curve of CNCs as a function of varying pH and NaOH volume

Conductivity and sulfur content of CNCs

In order to determine the sulfur content of CNCs obtained via acid hydrolysis, conductometric titration of the CNCs was performed as a function of varying pH values and amount of NaOH. The curve obtained from conductometric titration of CNCs is shown in Figure 3. The conductivity of CNCs at the neutralization point (~ 0.23 mL of NaOH and pH of about 5) was found as 193.74 ($\mu\text{S}/\text{cm}$) and the sulfur content was calculated as 1.82% , according to Equation (2). Jordan *et al.*⁵⁴ calculated the sulfur content of cotton gin motes and cotton gin waste CNCs to be between 0.05 - 1.04% . Similarly, Chen *et al.*⁵⁵ determined the sulfur content of bleached eucalyptus kraft pulp CNCs as 3 - 10 mg/g. In another study, Lin and Dufresne⁵⁶ found the sulfur content of filter paper CNCs between 0.18 - 1.31% . As a consequence, the sulfur ratio of CNCs decreased, as sulfuric acid was removed from CNCs successfully.

Morphological properties

Figure 4 shows optical microscopy images of fiber solutions for different grinding repetitions in the production of CNFs and agglomerated CNCs. Observing the microscopy images, it can be seen that, as the number of grinding repetitions of bleached sunflower stalk pulp in the grinder increased, the pulp defibrillated more and the dimensions of the fibers diminished gradually.

In Figure 5, SEM and S/TEM images of the raw material, bleached fibers, CNFs and CNCs are presented. Figure 5 (B1, B2 and B3) confirms that hemicelluloses and lignin were removed from the raw material after maceration and bleaching treatments. In addition, it was proved that micro-sized fibers converted to CNFs via high defibrillation after grinding via SEM analysis (Fig. 5C1, 5C2, 5C3) and S/TEM analysis (Fig. 5C4, 5C5, 5C6).

S/TEM images reveal the difference between CNFs and CNCs (Fig. 5C4, 5C5, 5C6, 5D1, 5D2 and 5D3). These images are in agreement with others reported in the literature. CNFs had a reticular structure in the wake of mechanical grinding, while CNCs had a needle-like structure with the removal of the amorphous parts from the fibers, thanks to sulphuric acid hydrolysis treatment. Besides, some agglomerations occurred in the CNC solution according to Figure 5D1 and D2.

The average fiber widths of the raw material, bleached fiber, CNFs and CNCs were found as 109.65 μm , 12.18 μm , 15.03 ± 3.68 nm and 13.91 ± 3.09 nm, respectively. Besides, the average length of CNCs was calculated as 60.44 ± 21.06 nm. Many studies have reported on the dimensions of cellulose nanomaterials produced from different natural resources, biomass and wastes. Sucharitpong *et al.*⁵⁷ extracted CNCs from sugarcane bagasse and they found the diameter and length of the obtained CNCs as 52.4 ± 14.8 and 400.38 ± 104.8 nm, respectively. Thakur *et al.*⁵⁸ found the average diameter of CNCs produced from rice straw derived from α -cellulose in the range of 5 - 15 nm. In another study, Debiagi *et al.*⁵⁹ measured the diameters of soybean hull CNFs to be approximately 80 - 100 nm. Marinho *et al.*⁶⁰ achieved CNFs from ramie fibers and their average thickness was found as 8.72 nm. Krishnadev *et al.*⁶¹ confirmed that the average particle size of *Agave americana* L. CNFs was 18.2 nm \pm 10.14 nm. Ramakrishnan *et al.*⁶² found the average diameter and length of CNCs produced from cotton as 18.4 ± 7.2 nm and 297.7 ± 98.9 nm, respectively. Yan *et al.*⁶³ obtained rice straw CNFs with widths of 30 - 200 nm and Bharimalla *et al.*⁶⁴ produced CNFs with a diameter in the range of 50 to 200 nm from bleached cotton linter pulp. In another study, Istomin *et al.*⁶⁵ extracted CNCs from flax

stalks. They found that the average diameter and length of CNCs were 85 ± 39 nm and 158 ± 89 nm, respectively.

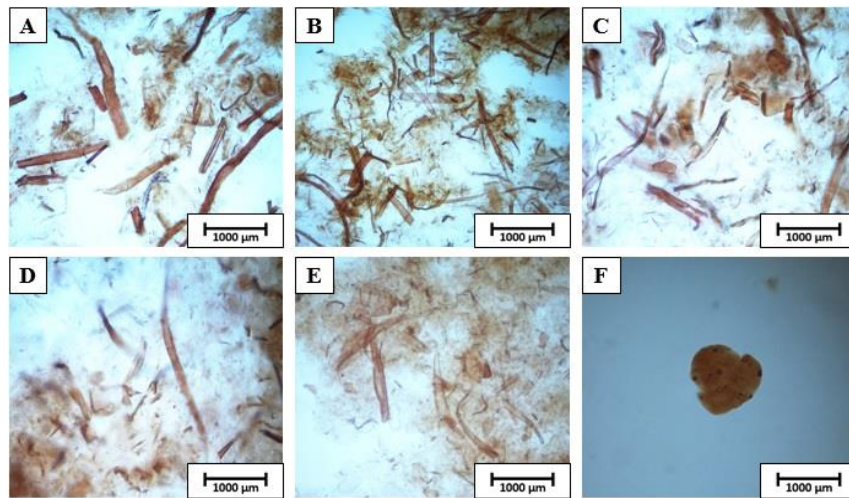


Figure 4: Optical microscopy images of fiber solutions for different numbers of grinding repetitions in the production of CNFs, (A) 1st, (B) 2nd, (C) 3rd, (D) 4th, (E) 5th, and (F) agglomerated CNCs

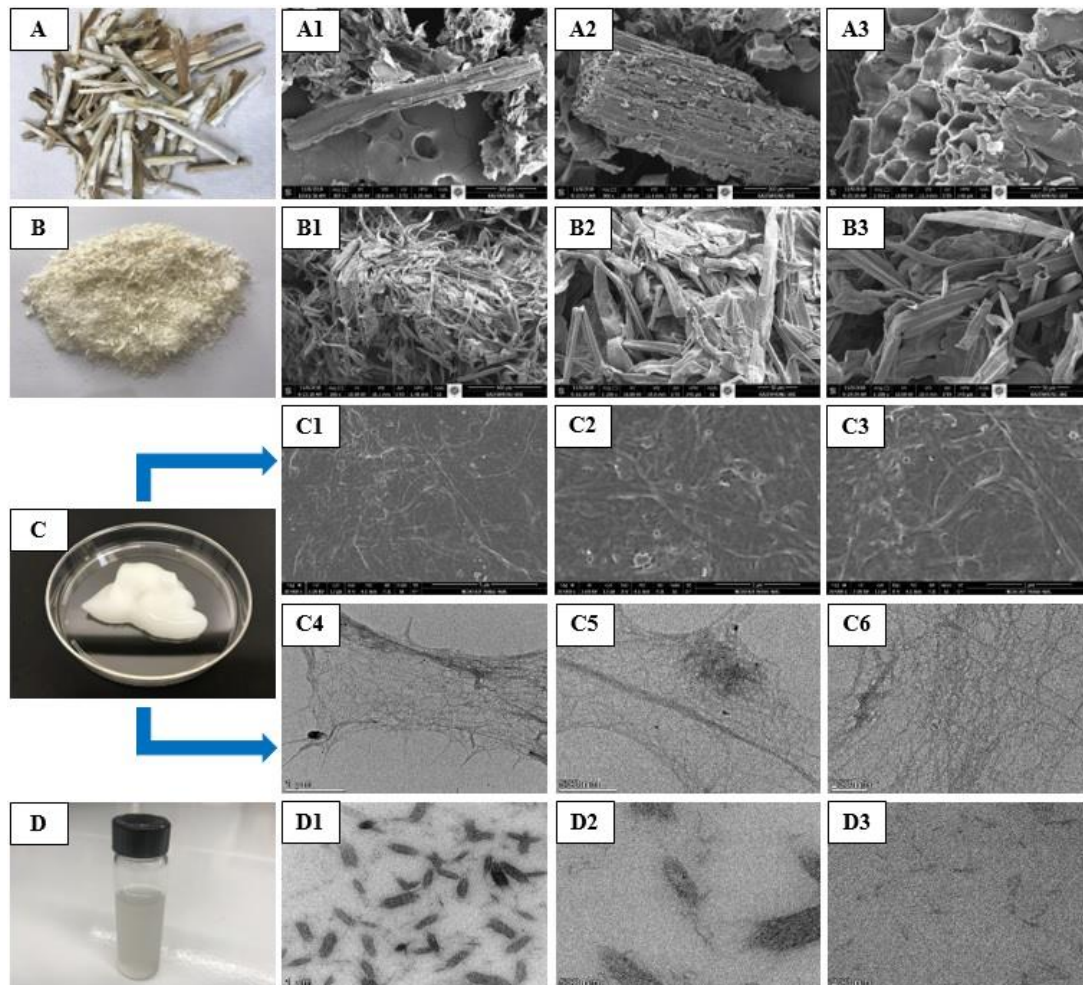


Figure 5: (A) Raw material, (A1), (A2), (A3) SEM images of raw material; (B) Bleached fibers, (B1), (B2), (B3) SEM images of bleached fibers; (C) CNF, (C1), (C2), (C3) SEM images of CNF, (C4), (C5), (C6) S/TEM images of CNF; (D) CNC, (D1), (D2), (D3) S/TEM images of CNC

Crystallinity

The crystallinity index of the raw material, bleached fiber, CNFs and CNCs was found as 55.07%, 77.34%, 82.64% and 83.09%, respectively. Because the raw material contained hemicelluloses and lignin components, besides cellulose, the crystalline regions of cellulose occupied very little space in the total material. Therefore, the crystallinity index of the raw material had the lowest value among all the samples. The crystallinity index of the samples increased step by step as a result of fibrillation, purification, delignification and removal of amorphous zones with maceration, bleaching, grinding and acid hydrolysis treatments. The crystallinity index of CNFs and CNCs was higher than those of the raw material and bleached fiber, thanks to mechanical degradation and sulphuric acid treatment. During the grinding process performed at high speed, the bleached fibers in the grinder were exposed to a high shearing resistance between two stone discs, one stable and one moving. Thus, the fiber bundles were fragmented and CNFs with high crystallinity were released. The crystallinity index of CNCs stood out as the highest value, among those of the raw material, bleached fiber and CNF samples. The acid hydrolysis treatment applied to the bleached fibers removed the amorphous regions of cellulose and provided a high percentage of crystalline regions of cellulose in the suspension. The XRD results of all the samples are illustrated in Figure 6.

The crystallinity of nanocellulose obtained from different agricultural and industrial products, as well as their residues, is much discussed in the literature. For instance, Zhong *et al.*⁶⁶ produced CNFs and CNCs from recycled indigo-dyed denim fabric and bleached cotton fabric with TEMPO modification/mechanical disintegration and sulfuric acid hydrolysis, respectively. They found crystallinity indices of CNFs of 66% and 71.6% for indigo-dyed denim fabric and bleached cotton fabric, respectively, whereas for CNCs – crystallinity indices of 85.6% for indigo-dyed denim fabric and 86.4% for bleached cotton fabric. Kian *et al.*⁶⁷ obtained CNCs from olive fibers with different hydrolysis reaction times of 30 min, 45 min and 60 min. They determined the crystallinity index of olive fiber CNCs as 74.8%, 79.8% and 83.1% for samples treated during 30 min, 45 min and 60 min, respectively. Salari *et al.*⁶⁸ found the crystallinity index of sugar beet molasse CNCs as 87.63%, while that of cheese whey media CNCs as 73.55%. Ilyas *et al.*⁵² obtained CNFs from sugar palm with high pressure homogenization treatment at 3 different numbers of cycles – of 5, 10 and 15 cycles. It was determined that the crystallinity indices of CNFs obtained after the 5, 10 and 15 cycle processes were 75.73%, 75.38% and 81.19%, respectively.

Thermal properties

The TGA curves of the raw material, bleached fiber, CNCs and CNFs are shown in Figure 7. The initial weight loss of approximately 5% in the raw material and bleached fiber samples up to 100 °C was due to the evaporation of moisture from these samples. Because the moisture in the freeze-dried CNF sample was removed before thermal analysis, no mass loss was observed up to 100 °C for this sample. The reason why there was no significant weight loss up to 100 °C in CNCs was that sulfuric acid used in the production of CNCs was a strong water retaining chemical and therefore the moisture in the sample could not evaporate completely. The main degradation of the samples occurred between 240-370 °C for the raw material, 220-370 °C for bleached fiber, 200-300 °C and 300-500 °C for CNFs, as well as 290-420 °C for CNCs. Although CNFs started to decompose at lower temperature compared to the others, it remained more stable and the weight loss at high temperature was lower. It was determined that the degradation of the CNF sample happened in two stages. There was a weight loss of about 35% in the first degradation stage, which occurred between 200-300 °C, and a weight loss of about 30% in the second degradation stage between 300-500 °C. However, it was determined that the weight loss in the second degradation stage took place with a lower acceleration than the others. When the CNC sample was investigated, it was determined that it started to decompose at a higher temperature (290 °C), compared to the other samples, and the degradation continued up to high temperature (approximately 420 °C), due to its strong crystalline structure and high crystallinity index. By means of TGA, it was proved that the CNCs and CNFs exhibited enhanced thermal properties. In addition, the char residues were determined as 22.11% for the raw material, 18.25% for bleached fiber, 18.44% for CNCs and 25.03% for CNFs.

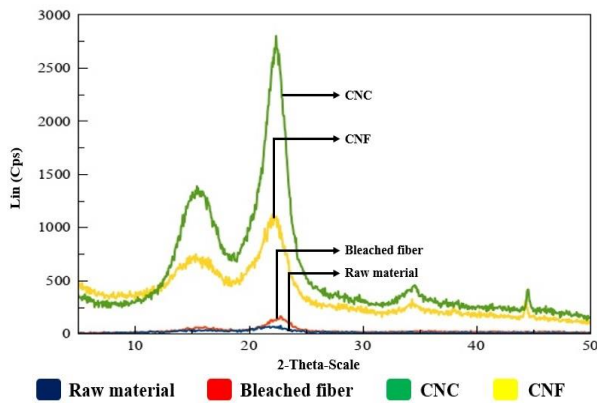


Figure 6: XRD patterns of raw material, bleached fiber, CNFs and CNCs

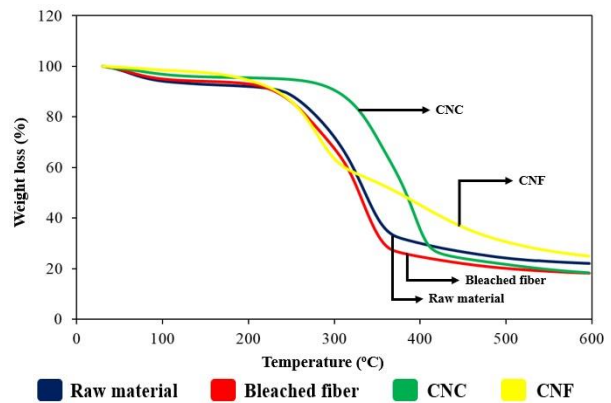


Figure 7: TGA curves of raw material, bleached fiber, CNFs and CNCs

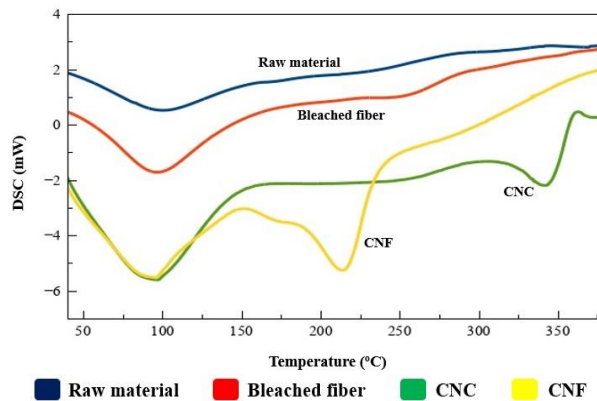


Figure 8: DSC curves of raw material, bleached fiber, CNFs and CNCs

A literature review revealed that the thermal degradation of CNFs and CNCs is generally reported to occur at high temperature. Patel and Joshi⁶⁹ obtained CNFs from banana fibers by using *Trichoderma reesei* cellulase enzyme. They found the thermal degradation temperature of CNFs to be between 300-425 °C. Supian *et al.*⁷⁰ determined that the thermal degradation of CNFs produced from empty fruit bunch via the mechanical method started at 200 °C and reached 350 °C. In another study, Hemmati *et al.*⁷¹ extracted CNCs, independently varying different parameters, such as sulfuric acid concentration, homogenization speed and duration. The researchers found the thermal degradation of CNCs to be between 130 °C and 420 °C. Kamelnia *et al.*⁷² produced CNCs from *Ferula gummosa*. They observed the main degradation of the raw material at 449 °C, with the weight loss of 23 wt%, whereas that of CNCs – at 500 °C with the weight loss of 43 wt%. Ahuja *et al.*⁷³ achieved CNFs from waste jute bags and they specified the first degradation temperature and the main degradation temperature of CNFs as 250 °C and 360 °C, respectively.

In Figure 8, the DSC results of the raw material, bleached fiber, CNCs and CNFs are shown. The endothermic peaks seen around 100 °C in all the samples were caused by the evaporation of absorbed moisture for the raw material and bleached fiber samples, whereas it was thought that the endothermic peaks here may be due to the glass transition temperature of CNFs and CNCs or other thermo-mechanical properties, because no moisture loss could be detected in the CNF and CNC samples around this temperature.⁷⁴ The peak in the range of 200-250 °C in the CNF explained the first thermal degradation of this sample.⁷³ In the DSC curve of CNF, the peak describing the first degradation was seen as a distinct endothermic peak, while the second degradation that occurred with low acceleration was detected with a decreasing curve. In the CNC sample, the peak observed between 325 °C and 360 °C indicated the main thermal degradation of this sample.⁷⁵ Although the CNC and CNF samples were compatible with each other in TGA and DSC analyses in terms of main degradation temperature ranges, the thermal degradation occurring between 240-370 °C and 220-370 °C in the TGA graph for the raw material and bleached fiber samples, respectively, could not be detected in the DSC graph. This can be explained by the increase in the crystallinity of these materials as a result of the chemical and mechanical methods applied in the production of CNCs and CNFs.⁷⁶

Chemical bond structures

The FTIR analysis was performed to determine the chemical bond structure for all the samples. The FTIR results of the samples (raw material, bleached fiber, CNFs and CNCs), are presented in Figure 9.

The peak at 3337 cm^{-1} represented the intramolecular O–H bond,⁷⁷ while the peaks at 2981 cm^{-1} and at 2869 cm^{-1} represented the aliphatic C–H bond⁷⁸ in the raw material. The vibration at 1737 cm^{-1} was attributed to acetyl and uronic ester groups (C=O) from hemicelluloses or the ester bond (C=O) of the carboxylic groups in ferulic and p-coumaric acids of lignin or hemicelluloses.⁷⁹ In addition, the peak at 1503 cm^{-1} represented the aromatic C=C vibration due to the aromatic ring of lignin.⁷⁹ The peaks at 1421 cm^{-1} , 1368 cm^{-1} , 1319 cm^{-1} and 1079 cm^{-1} reflected typical C–H bonds of the cellulose in the raw material sample.⁸⁰ The peak at 1232 cm^{-1} was related to lignin and it represented the C–O–C bond, which is commonly observed in ether, ester and phenol groups.⁷⁹ The vibration observed at 1028 cm^{-1} corresponded to the C–O–C linkage of the pyranose ring.⁴⁸

For the bleached fiber sample, the peaks at 3298 cm^{-1} and 2893 cm^{-1} were attributed to intramolecular O–H bonds in cellulose⁴⁸ and C–H bond for alkane,³⁹ respectively. The vibration at 1720 cm^{-1} was due to the acetyl and uronic ester groups (C=O) in residual hemicelluloses after the bleaching treatment.⁸¹ However, the vibrations detected at 1503 cm^{-1} and 1232 cm^{-1} in the raw material, indicating the presence of lignin, were not observed in the bleached fiber sample. This situation revealed that lignin was completely removed from the raw material as a result of maceration and bleaching processes. The vibrations at 1420 cm^{-1} , 1332 cm^{-1} and 1314 cm^{-1} represented typical C–H bonds of cellulose.⁸⁰ The peak that emerges at 1155 cm^{-1} demonstrated asymmetric C–O–C linkage of cellulose.⁴⁸ In addition, the peaks determined at 1095 cm^{-1} , 1051 cm^{-1} and 1010 cm^{-1} were attributed to the carbohydrate rings of the cellulose skeleton.⁸²

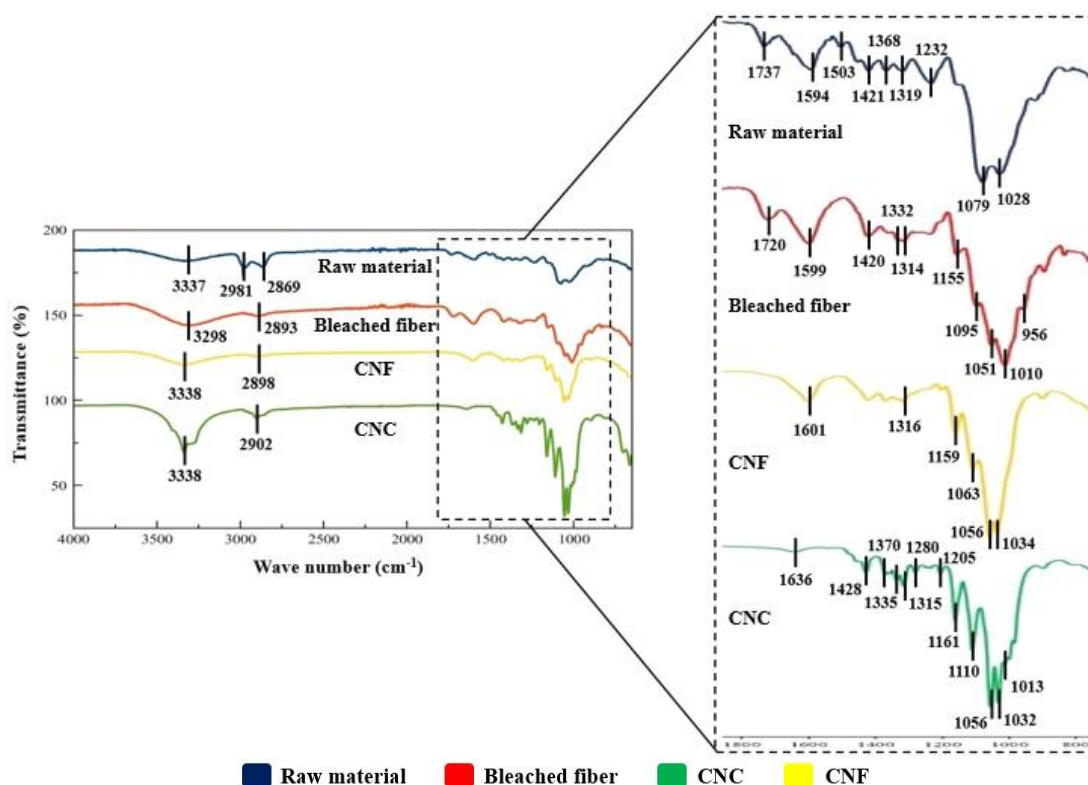


Figure 9: FTIR spectra of raw material, bleached fiber, CNCs and CNFs

In the CNF sample, the peak observed at 3338 cm^{-1} represented the intramolecular O–H bond.⁸³ The peak at 2898 cm^{-1} showed symmetric and asymmetric C–H bond,⁸² while the peak at 1601 cm^{-1} was attributed to the O–H bond of absorbed water in cellulose.⁶¹ The vibrations reflecting hemicelluloses and lignin detected at 1737 cm^{-1} , 1503 cm^{-1} and 1232 cm^{-1} in the raw material were not observed in the CNFs. Thus, it was proven that the production of CNFs was successfully performed by

removing lignin and hemicelluloses from the raw material and bleached fiber samples completely. The peaks determined at 1316 cm^{-1} , 1159 cm^{-1} and 1063 cm^{-1} reflected the C–H linkage,⁸⁰ asymmetric C–O–C linkage⁴⁸ and C–O linkage in C3 position⁸⁴ of cellulose, respectively. Furthermore, it was confirmed that the peaks at 1056 cm^{-1} and 1034 cm^{-1} belonged to carbohydrate rings in the cellulose structure.⁸²

The peak detected at 3338 cm^{-1} represented the intramolecular O–H bond in CNCs.³⁹ The vibrations at 2902 cm^{-1} and 1428 cm^{-1} expressed the aliphatic C–H bond in the methylene groups of cellulose⁸⁵ and the symmetric CH_2 structure in the cellulose structure,⁸⁶ respectively. The peak observed at 1370 cm^{-1} indicated C–H linkage.⁸⁷ The vibrations at 1315 cm^{-1} and 1280 cm^{-1} reflected C–H and C–O bonds in the polysaccharide rings.⁸⁸ It was observed that the ester bond (C=O) vibrations, which reflect lignin and hemicelluloses in the raw material and bleached fiber samples, completely disappeared in CNCs and CNFs. This showed that lignin and hemicelluloses were completely removed as a result of maceration, bleaching and acid hydrolysis processes and CNC production was carried out successfully. The peak determined at 1636 cm^{-1} was attributed the O–H bond of the absorbed water.⁸⁶ The vibration occurring at 1335 cm^{-1} belonged to the C–H structure, showing the hydrogen bonds between CNCs.³⁹ The peak at 1205 cm^{-1} referred to sulfate groups formed *via* sulfuric acid hydrolysis.⁸⁹ The peak at 1161 cm^{-1} reflected ring C–C linkage, whereas the peak at 1110 cm^{-1} indicated C–O–C glycosidic ether linkage.⁹⁰ The peaks seen at 1056 cm^{-1} , 1032 cm^{-1} and 1013 cm^{-1} were attributed to asymmetric vibrations in the $\text{C}_1\text{--O--C}_4$ structure, asymmetric vibrations in the pyranose ring and C–O bonds.⁹¹

CONCLUSION

In this study, sunflower stalks were evaluated in the production of CNCs and CNFs. The mechanical process for the production of CNFs and the chemical treatment for obtaining CNCs were performed successfully. Needle-shaped CNCs and spaghetti-shaped CNFs were produced with these methods. As the dimensions of the samples approached the nano-scale, the turbidity values decreased, while zeta potential increased. It was found that the crystallinity indices of CNCs and CNFs were higher than those of the raw material and bleached fibers. Besides, it was determined that the thermal properties of CNCs and CNFs were superior to those of the other samples. As a result of FTIR spectroscopy, the bond structures of all the samples were characterized. To sum up, it was demonstrated that, as a waste bio-material, sunflower stalks can be a suitable raw material for production of CNMs.

ACKNOWLEDGEMENT: The authors would like to acknowledge the Scientific and Technological Research Council of Turkey (Türkiye Bilimsel ve Teknolojik Araştırma Kurumu, Project #1059B141800332) for financial support, Dr. Marko Hakovirta who is Head of Department and Dr. Steve Kelley from the Department of Forest Biomaterials, North Carolina State University, for their collaboration and support, the technicians from Chemical Analysis and Spectroscopy Laboratory (CASL) in the Department of Forest Biomaterials and Analytical Instrumentation Facility (AIF), North Carolina State University, as well as from Mehmet Hakan Akyıldız Central Research Laboratory, Kastamonu University, for their assistance, Dr. Mahmut Gür from the Department of Forest Industrial Engineering and Dr. Serkan Islak from the Department of Mechanical Engineering, Kastamonu University, for their support.

REFERENCES

- ¹ M. Jonoobi, R. Oladi, Y. Davoudpour, K. Oksman, A. Dufresne *et al.*, *Cellulose*, **22**, 935 (2015), <https://doi.org/10.1007/s10570-015-0551-0>
- ² S. Mansouri, R. Khiari, F. Bettaieb, A. A. El-Gendy and F. Mhenni, *J. Polym. Environ.*, **23**, 190 (2015), <https://doi.org/10.1007/s10924-014-0691-6>
- ³ N. Olaru, L. Olaru, A. Stoleriu and D. Timpu, *J. Appl. Polym. Sci.*, **67**, 481 (1998), [https://doi.org/10.1002/\(SICI\)1097-4628\(19980118\)67:3<481::AID-APP11>3.0.CO;2-Z](https://doi.org/10.1002/(SICI)1097-4628(19980118)67:3<481::AID-APP11>3.0.CO;2-Z)
- ⁴ R. Khiari, E. Mauret, M. N. Belgacem and F. Mhemmi, *BioResources*, **6**, 265 (2011)
- ⁵ F. Kallel, F. Bettaieb, R. Khiari, A. García, J. Bras *et al.*, *Ind. Crop. Prod.*, **87**, 287 (2016), <https://doi.org/10.1016/j.indcrop.2016.04.060>
- ⁶ D. Klemm, B. Heublein, H.-P. Fink and A. Bohn, *Angew. Chem. Int.*, **44**, 3358 (2005), <https://doi.org/10.1002/anie.200460587>

- ⁷ C. Yan, J. Wang, W. Kang, M. Cui, X. Wang *et al.*, *Adv. Mater.*, **26**, 2022 (2014), <https://doi.org/10.1002/adma.201304742>
- ⁸ N. Lin and A. Dufresne, *Eur. Polym. J.*, **59**, 302 (2014), <https://doi.org/10.1016/j.eurpolymj.2014.07.025>
- ⁹ Z. Shi, X. Gao, M. W. Ullah, S. Li, Q. Wang *et al.*, *Biomaterials*, **111**, 40 (2016), <https://doi.org/10.1016/j.biomaterials.2016.09.020>
- ¹⁰ M. Ul-Islam, M. W. Ullah, S. Khan, T. Kamal, S. Ul-Islam *et al.*, *Recent Pat. Nanotechnol.*, **10**, 169 (2016), <https://doi.org/10.2174/1872210510666160429144916>
- ¹¹ A. Jasim, M. W. Ullah, Z. Shi, X. Lin and G. Yang, *Carbohydr. Polym.*, **163**, 62 (2017), <https://doi.org/10.1016/j.carbpol.2017.01.056>
- ¹² W. Czaja, A. Krystynowicz, S. Bielecki and R. M. Brown, *Biomaterials*, **27**, 145 (2006), <https://doi.org/10.1016/j.biomaterials.2005.07.035>
- ¹³ R. J. Moon, A. Martini, J. Nairn, J. Simonsen and J. Youngblood, *Chem. Soc. Rev.*, **40**, 3941 (2011), <https://doi.org/10.1039/C0CS00108B>
- ¹⁴ N. Shah, M. Ul-Islam, W. A. Khatkhatk and J. K. Park, *Carbohydr. Polym.*, **98**, 1585 (2013), <https://doi.org/10.1016/j.carbpol.2013.08.018>
- ¹⁵ ISO/TS 20477. Nanotechnologies – Standard terms and their definition for cellulose nanomaterial (2017), <https://www.iso.org/standard/68153.html>
- ¹⁶ S. H. Osong, S. Norgren and P. Engstrand, *Cellulose*, **23**, 93 (2016), <https://doi.org/10.1007/s10570-015-0798-5>
- ¹⁷ K. Kekäläinen, H. Liimatainen and J. Niinimäki, *Cellulose*, **21**, 3691 (2014), <https://doi.org/10.1007/s10570-014-0363-7>
- ¹⁸ K. Kekäläinen, H. Liimatainen, M. Illikainen, T. C. Maloney and J. Niinimäki, *Cellulose*, **21**, 1163 (2014), <https://doi.org/10.1007/s10570-014-0210-x>
- ¹⁹ K. Uetani and H. Yano, *Biomacromolecules*, **12**, 348 (2011), <https://doi.org/10.1021/bm101103p>
- ²⁰ L. Wågberg, G. Decher, M. Norgren, T. Lindström, M. Ankerfors *et al.*, *Langmuir*, **24**, 784 (2008), <https://doi.org/10.1021/la702481v>
- ²¹ M. Henriksson, G. Henriksson, L. A. Berglund and T. Lindström, *Eur. Polym. J.*, **43**, 3434 (2007), <https://doi.org/10.1016/j.eurpolymj.2007.05.038>
- ²² M. A. Hubbe, O. J. Rojas, L. A. Lucia and M. Sain, *BioResources*, **3**, 929 (2008)
- ²³ A. García, A. Gandini, J. Labidi, N. Belgacem and J. Bras, *Ind. Crop. Prod.*, **93**, 26 (2016), <https://doi.org/10.1016/j.indcrop.2016.06.004>
- ²⁴ J. Huang, X. Ma, G. Yang and A. Dufresne, in “Nanocellulose: From Fundamentals to Advanced Materials”, edited by J. Huang, A. Dufresne and N. Lin, Wiley-WCH, Weinheim, Germany, 2019, pp. 1-15
- ²⁵ A. Demirel, Master’s Thesis, Ahi Evran University, Institute of Science, Kırşehir, 2004
- ²⁶ V. Marechal and L. Rigal, *Ind. Crop. Prod.*, **10**, 185 (1999), [https://doi.org/10.1016/S0926-6690\(99\)00023-0](https://doi.org/10.1016/S0926-6690(99)00023-0)
- ²⁷ TAPPI Test Method T257, Sampling and preparing wood for analysis, (2014), https://www.techstreet.com/standards/tappi-t257-sp-14?product_id=1877258
- ²⁸ TAPPI Test Method T204, Solvent extractives of wood and pulp, (2007), <https://www.tappi.org/content/sarg/t204.pdf>
- ²⁹ L. E. Wise, M. Murphy and A. A. D’Adieco, *Pap. Trade J.*, **122**, 35 (1946)
- ³⁰ TAPPI Test Method T203, Alpha-, beta- and gamma-cellulose in pulp, (2009), <https://imisrise.tappi.org/TAPPI/Products/01/T/0104T203.aspx>
- ³¹ TAPPI Test Method T222, Acid-insoluble lignin in wood and pulp, (2002), <https://imisrise.tappi.org/TAPPI/Products/01/T/0104T222.aspx>
- ³² TAPPI Test Method T211, Ash in wood, pulp, paper and paperboard: combustion at 525°C, (2007), <https://www.tappi.org/content/sarg/t211.pdf>
- ³³ TAPPI Test Method T207, Water solubility of wood and pulp, (2008), https://infostore.saiglobal.com/en-us/Standards/TAPPI-T-207-2008-1062596_SAIG_TAPPI_TAPPI_2471555/
- ³⁴ TAPPI Test Method T212, One percent sodium hydroxide solubility of wood and pulp, (2012), <https://imisrise.tappi.org/TAPPI/Products/01/T/0104T212.aspx>
- ³⁵ S. Mahesh, P. Kumar and S. A. Ansari, *Trop. Plant Res.*, **2**, 108 (2015)
- ³⁶ F. Gu, W. Wang, Z. Cai, F. Xue, Y. Jin *et al.*, *Cellulose*, **25**, 2861 (2018), <https://doi.org/10.1007/s10570-018-1765-8>
- ³⁷ TAPPI Test Method T248, Laboratory beating of pulp (PFI mill method), (2015), <https://imisrise.tappi.org/TAPPI/Products/01/T/0104T248.aspx>
- ³⁸ TAPPI Test Method T227, Freeness of Pulp (Canadian Standard Method), (2017), <https://imisrise.tappi.org/TAPPI/Products/01/T/0104T227.aspx>
- ³⁹ V. F. Korolovych, V. Cherpak, D. Nepal, A. Ng, N. R. Shaikh *et al.*, *Polymer*, **145**, 334 (2018), <https://doi.org/10.1016/j.polymer.2018.04.064>

- ⁴⁰ K. Kriechbaum, P. Munier, V. Apostolopoulou-Kalkavoura and N. Lavoine, *ACS Sustain. Chem. Eng.*, **6**, 11959 (2018), <https://doi.org/10.1021/acssuschemeng.8b02278>
- ⁴¹ X. M. Dong, J. F. Revol and D. G. Gray, *Cellulose*, **5**, 19 (1998), <https://doi.org/10.1023/A:1009260511939>
- ⁴² N. Reddy and Y. Yang, *Polymer*, **46**, 5494 (2005). <https://doi.org/10.1016/j.polymer.2005.04.073>
- ⁴³ S. Ateş, İ. Deniz, H. Kırcı, C. Atik and O. T. Okan, *Turk. J. Agric. For.*, **39**, 144 (2015), <https://doi.org/10.3906/tar-1403-41>
- ⁴⁴ Ş. Bostancı, Thesis of Associate Professor, Karadeniz Technical University, Faculty of Forestry, Trabzon (1980)
- ⁴⁵ J. Desmays, E. Boutonnet, M. Rueff, A. Dufresne and J. Bras, *Carbohydr. Polym.*, **174**, 318 (2017), <https://doi.org/10.1016/j.carbpol.2017.06.032>
- ⁴⁶ K. Pacaphol, K. Seraypheap and D. Aht-Ong, *Carbohydr. Polym.*, **224**, 115167 (2019), <https://doi.org/10.1016/j.carbpol.2019.115167>
- ⁴⁷ M. El Achaby, Z. Kassab, A. Aboulkas, C. Gaillard and A. Barakat, *Int. J. Biol. Macromol.*, **106**, 681 (2018), <https://doi.org/10.1016/j.ijbiomac.2017.08.067>
- ⁴⁸ M. El Achaby, N. El Miri, H. Hannache, S. Gmouh, H. Ben Youcef *et al.*, *Int. J. Biol. Macromol.*, **117**, 592 (2018), <https://doi.org/10.1016/j.ijbiomac.2018.05.201>
- ⁴⁹ M. El Achaby, Z. Kassab, A. Barakat and A. Aboulkas, *Ind. Crop. Prod.*, **112**, 499 (2018), <https://doi.org/10.1016/j.indcrop.2017.12.049>
- ⁵⁰ K. Oh, S. Kwon, W. Xu, X. Wang and M. Toivakka, *Cellulose*, **27**, 5003 (2020), [https://doi.org/10.1016/S0377-0257\(98\)00206-7](https://doi.org/10.1016/S0377-0257(98)00206-7)
- ⁵¹ S. Josset, P. Orsolini, G. Siqueria, A. Tejado, P. Tingaut *et al.*, *Nord. Pulp Pap. Res. J.*, **29**, 167 (2014)
- ⁵² R. A. Ilyas, S. M. Sapuan, M. R. Ishak and E. S. Zainudin, *Int. J. Biol. Macromol.*, **123**, 379 (2019), <https://doi.org/10.1016/j.ijbiomac.2018.11.124>
- ⁵³ P. L. M. Ribeiro, T. V. B. Figueiredo, L. E. Moura and J. I. Druzian, *Polym. Adv. Technol.*, **30**, 573 (2018), <https://doi.org/10.1002/pat.4494>
- ⁵⁴ J. H. Jordan, M. W. Easson, B. Dien, S. Thompson and B. D. Condon, *Cellulose*, **26**, 5959 (2019), <https://doi.org/10.1007/s10570-019-02533-7>
- ⁵⁵ L. Chen, Q. Wang, K. Hirth, C. Baez, U. P. Agarwal *et al.*, *Cellulose*, **22**, 1753 (2015), <https://doi.org/10.1007/s10570-015-0615-1>
- ⁵⁶ N. Lin and A. Dufresne, *Nanoscale*, **6**, 5384 (2014), <https://doi.org/10.1039/C3NR06761K>
- ⁵⁷ T. Sucharitpong, N. T. Lam and P. Sukyai, *Sugar Tech*, **22**, 328 (2020), <https://doi.org/10.1007/s12355-019-00775-0>
- ⁵⁸ M. Thakur, A. Sharma, V. Ahlawat, M. Bhattacharya and S. Goswami, *Mater. Sci. Technol.*, **3**, 328 (2020), <https://doi.org/10.1016/j.mset.2019.12.005>
- ⁵⁹ F. Debiagi, P. C. S. Faria-Tischer and S. Mali, *Cellulose*, **27**, 1975 (2020), <https://doi.org/10.1007/s10570-019-02893-0>
- ⁶⁰ N. P. Marinho, P. H. G. de Cademartori, S. Nisgoski, V. O. de Andrade Tanobe, U. Klock *et al.*, *Carbohydr. Polym.*, **230**, 115579 (2020), <https://doi.org/10.1016/j.carbpol.2019.115579>
- ⁶¹ P. Krishnadev, K. S. Subramanian, G. J. Janavi, S. Ganapathy and A. Lakshmanan, *BioResources*, **15**, 2442 (2020)
- ⁶² A. Ramakrishnan, K. Ravishankar and R. Dhamodharan, *Cellulose*, **26**, 3127 (2019), <https://doi.org/10.1007/s10570-019-02312-4>
- ⁶³ J. Yan, J. Hu, R. Yang, Z. Zhang and W. Zhao, *ACS Sustain. Chem. Eng.*, **6**, 3481 (2018), <https://doi.org/10.1021/acssuschemeng.7b03765>
- ⁶⁴ A. K. Bharimalla, P. G. Patil, S. P. Deshmukh and N. Vigneshwaran, *Cellulose Chem. Technol.*, **51**, 395 (2017), [https://www.cellulosechemtechnol.ro/pdf/CCT5-6\(2017\)/p.395-401.pdf](https://www.cellulosechemtechnol.ro/pdf/CCT5-6(2017)/p.395-401.pdf)
- ⁶⁵ A. V. Istomin, T. S. Demina, E. N. Subcheva, T. A. Akopova and A. N. Zelenetskii, *Fibre Chem.*, **48**, 199 (2016), <https://doi.org/10.1007/s10692-016-9767-5>
- ⁶⁶ T. Zhong, R. Dhandapani, D. Liang, J. Wang, M. P. Wolcott *et al.*, *Carbohydr. Polym.*, **240**, 116283 (2020), <https://doi.org/10.1016/j.carbpol.2020.116283>
- ⁶⁷ L. K. Kian, N. Saba, M. Jawaid, O. Y. Alothman and H. Fouad, *Carbohydr. Polym.*, **241**, 116423 (2020), <https://doi.org/10.1016/j.carbpol.2020.116423>
- ⁶⁸ M. Salari, M. S. Khiabani, R. R. Mokarram, B. Ghanbarzadeh and H. S. Kafil, *Int. J. Biol. Macromol.*, **122**, 280 (2019), <https://doi.org/10.1016/j.ijbiomac.2018.10.136>
- ⁶⁹ B. H. Patel and P. V. Joshi, *J. Package Technol. Res.*, **4**, 95 (2020), <https://doi.org/10.1007/s41783-020-00083-z>
- ⁷⁰ M. A. F. Supian, K. N. M. Amin, S. S. Jamari and S. Mohamad, *J. Environ. Chem. Eng.*, **8**, 103024 (2020), <https://doi.org/10.1016/j.jece.2019.103024>
- ⁷¹ F. Hemmati, S. M. Jafari and R. A. Taheri, *Int. J. Biol. Macromol.*, **137**, 374 (2019), <https://doi.org/10.1016/j.ijbiomac.2019.06.241>

- ⁷² E. Kamelnia, A. Divsalar, M. Darroudi, P. Yaghmaei and K. Sadri, *Ind. Crop. Prod.*, **139**, 111538 (2019), <https://doi.org/10.1016/j.indcrop.2019.111538>
- ⁷³ D. Ahuja, A. Kaushik and M. Singh, *Int. J. Biol. Macromol.*, **107**, 1294 (2018), <https://doi.org/10.1016/j.ijbiomac.2017.09.107>
- ⁷⁴ X. Miao, J. Lin, F. Tian, X. Li, F. Bian *et al.*, *Carbohydr. Polym.*, **136**, 841 (2016), <https://doi.org/10.1016/j.carbpol.2015.09.056>
- ⁷⁵ Z. Wang, Z. Yao, J. Zhou and Y. Zhang, *Carbohydr. Polym.*, **157**, 945 (2017), <https://doi.org/10.1016/j.carbpol.2016.10.044>
- ⁷⁶ S. Maiti, J. Jayaramudu, K. Das, S. M. Reddy, R. Sadiku *et al.*, *Carbohydr. Polym.*, **98**, 562 (2013), <https://doi.org/10.1016/j.carbpol.2013.06.029>
- ⁷⁷ Z. Jahan, M. B. K. Niazi and Ø. W. Gregersen, *J. Ind. Eng. Chem.*, **57**, 113 (2018), <https://doi.org/10.1016/j.jiec.2017.08.014>
- ⁷⁸ S. Kyle, Z. M. Jessop, A. Al-Sabah, K. Hawkins, A. Lewis *et al.*, *Carbohydr. Polym.*, **198**, 270 (2018), <https://doi.org/10.1016/j.carbpol.2018.06.091>
- ⁷⁹ M. L. Foo, K. W. Tan, T. Y. Wu, E. S. Chan and I. M. L. Chew, *Chem. Eng. Trans.*, **60**, 97 (2017), <https://doi.org/10.3303/CET1760017>
- ⁸⁰ K. Xu, C. Liu, K. Kang, Z. Zheng, S. Wang *et al.*, *Compos. Sci. Technol.*, **154**, 8 (2018), <https://doi.org/10.1016/j.compscitech.2017.10.022>
- ⁸¹ R. A. Ilyas, S. M. Sapuan and M. R. Ishak, *Carbohydr. Polym.*, **181**, 1038 (2018), <https://doi.org/10.1016/j.carbpol.2017.11.045>
- ⁸² H. Khanjanzadeh, R. Behrooz, N. Bahramifar, W. Gindl-Altmutter, M. Bacher *et al.*, *Int. J. Biol. Macromol.*, **106**, 1288 (2018), <https://doi.org/10.1016/j.ijbiomac.2017.08.136>
- ⁸³ M. Jonoobi, J. Harun, A. Shakeri, M. Misra and K. Oksman, *BioResources*, **4**, 626 (2009)
- ⁸⁴ Y. Tang, X. Zhang, R. Zhao, D. Guo and J. Zhang, *Carbohydr. Polym.*, **197**, 128 (2018), <https://doi.org/10.1016/j.carbpol.2018.05.073>
- ⁸⁵ J. Lamaming, R. Hashim, O. Sulaiman, C. P. Leh, T. Sugimoto *et al.*, *Carbohydr. Polym.*, **127**, 202 (2015), <https://doi.org/10.1016/j.carbpol.2015.03.043>
- ⁸⁶ A. Kumar, Y. S. Negi, V. Choudhary and N. K. Bhardwaj, *JMPC*, **2**, 1 (2014), <https://doi.org/10.12691/jmpc-2-1-1>
- ⁸⁷ Y. Zhang, Y. Liu, R. Li, X. Ren and T. S. Huang, *J. Appl. Polym. Sci.*, **136**, 1 (2019), <https://doi.org/10.1002/app.47101>
- ⁸⁸ E. Hafemann, R. Battisti, D. Bresolin, C. Marangoni and R. A. F. Machado, *Waste Biomass Valor.*, **11**, 6595 (2020), <https://doi.org/10.1007/s12649-020-00937-2>
- ⁸⁹ K. Song, X. Zhu, W. Zhu and X. Li, *Bioresour. Bioprocess.*, **6**, 1 (2019), <https://doi.org/10.1186/s40643-019-0279-z>
- ⁹⁰ F. I. Ditzel, E. Prestes, B. M. Carvalho, I. M. Demiate and L. A. Pinheiro, *Carbohydr. Polym.*, **157**, 1577 (2017), <https://doi.org/10.1016/j.carbpol.2016.11.036>
- ⁹¹ E. Fortunati, D. Puglia, M. Monti, L. Peponi, C. Santulli *et al.*, *J. Polym. Environ.*, **21**, 319 (2013), <https://doi.org/10.1007/s10924-012-0543-1>